NUMERICAL SIMULATION OF VISCOUS FLOWS AROUND LIFTING BODIES OF COMPLICATED CONFIGURATION

A. Galaktionov, D. Fofonov

Keywords: *re-entry aerodynamics, CFD, flow separation region*

Abstract

One of the problems in manned space exploration is creation of new generation space vehicle (SV), which provide lateral manoeuvre about 500 km and comfort crew conditions at space vehicle descent trajectory. SV configuration of "lifting body" type satisfies these conditions. Known project "Klipper" is an example of such type configurations.

Principal part of the descent trajectory with respect to SV aerodynamic and heat loading is a region of hypersonic velocities. In this connection, numerical simulation of flows around the lifting body configurations like SV "Klipper" and others based on complete non-stationary Navier-Stocks equations is discussed. Turbulent flow regimes are analysed using κ-ε and Almaras turbulent models.

Particular attention is given to analysis of the influence of control surfaces and control jets on SV manoeuvring characteristics and maximum lift-to-drag ratio. Flow regimes with boundary layer separation in front of the deflected control surfaces/jets are examined.

Computational results are compared with experimental data. An approximate algorithm for numerical simulation of non-separated flow regimes based on local dependencies for pressure coefficients' estimation is suggested.

Computational results for hypersonic flows around the lifting body configurations with control surfaces/jets are presented.
A method for approximate numerical simulation of non-separated flow regimes is suggested

1 Introduction.

The main problem of modern manned flying is development of a safe aircraft to inject payload and men to orbits and to provide safe landing in different places. At the same time a wide circle of space tasks need to reduce the cost of payload injection, to provide given azimuth of flight and to increase of flight intensity to decrease time of preflight actions. These two tasks let examining the problem of manned flying aircraft as multi-criterion synthesis [1].

In this case the main meaning is aerodynamic scheme. Using the lift-to drag ratio (LDR) it is possible to provide the any-azimuth of flight and required azimuth deviation at re-entry flight trajectory [3, 6, 7].

The first studies [3, 4] of trajectories it was shown that hypersonic lift-to-drag ratio (K) about 3,23 ensures landing in every place of Earth. Required (minimum) lift-to-drag ratio for azimuth maneuver is K=0.5 [3].

The interval K from 0.5 to 3 is of the most interest and can be provided by the configurations as lifting body.

The main problem to choose configuration of the flight vehicle with lift-to-drag ratio in this interval is trade-off of flight controls and aerodynamic system vehicle-controls, because stability and controllability of hypersonic regime can provide the crew safety.

2 Comparison of aerodynamic schemes

Lift-to-drag ratio, efficiency of controls, and minimal expenditures were chosen as quantitative criteria of efficiency for modern manned aircraft.

For analysis of possible aerodynamic schemes it is convenient to use diagrams (Fig. 1) from [4]: $K = f(C_y/C_x)$. There are three groups here:

- capsule-type, with LDR up to 0,5 (type of "Souz", "Olympics", etc.), which can guarantee the safety of flight by possibility of ballistic re-entry trajectory,
- lifting body, with LDR up to 3 ("Clipper", X-24, X-30, etc.), with high requirements to efficiency of flight controls,
- flight vehicle with developed lifting surfaces ("Shuttle", "Buran", etc.), with LDR more then 3, and high requirements to thermal protection of construction.

If "Lifting body" aerodynamic scheme is chosen and center of gravity is located out of construction line of symmetry it is necessary for self-balance with high angles of attack to choose rationally flight controls and to find their characteristics especially for complicated configurations.

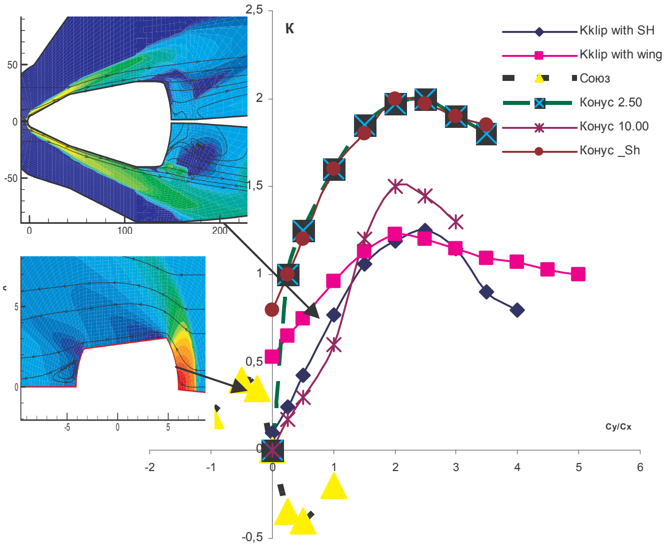

Fig.1. Different aerodynamic schemes

Taking into consideration that hypersonic regime can not be modeled at onground facilities, the numerical simulation is of great interest.

In this paper the main aerodynamic characteristics of re-entry models were obtained by computations of full Navier-Stokes equation.

$$\frac{\partial \sigma}{\partial t} + \frac{\partial a}{\partial x} + \frac{\partial b}{\partial y} + \frac{\partial c}{\partial z} = 0 \qquad (1)$$

where $\sigma = \begin{pmatrix} \rho \\ \rho u \\ \rho v \\ \rho w \\ e \end{pmatrix}$,

$$a = \begin{pmatrix} \rho u \\ \rho u^2 + p - \Omega_{xx} \\ \rho uv - \Omega_{yx} \\ \rho uw - \Omega_{zx} \\ (e+p)u - u\Omega_{xx} - v\Omega_{yx} - w\Omega_{zx} - \varsigma \frac{\partial T}{\partial x} \end{pmatrix},$$

$$b = \begin{pmatrix} \rho v \\ \rho uv - \Omega_{xy} \\ \rho v^2 + p - \Omega_{yy} \\ \rho uw - \Omega_{zy} \\ (e+p)v - u\Omega_{xy} - v\Omega_{yy} - w\Omega_{zy} - \varsigma \frac{\partial T}{\partial y} \end{pmatrix},$$

$$c = \begin{pmatrix} \rho w \\ \rho uw - \Omega_{xz} \\ \rho vw - \Omega_{yz} \\ \rho w^2 + p - \Omega_{zz} \\ (e+p)w - u\Omega_{xz} - v\Omega_{yz} - w\Omega_{zz} - \varsigma \frac{\partial T}{\partial z} \end{pmatrix}$$

$$\varsigma = \frac{1}{\mathrm{Re}_\infty \, \mathrm{Pr}_\infty},$$

$$e = \rho\left(\varepsilon + \frac{u^2 + v^2 + w^2}{2}\right)$$

$$\varepsilon = \frac{p}{(\gamma - 1)\rho}$$

Ω matrix structure:

$$\Omega = \begin{bmatrix} \nu\left(\frac{\partial u}{\partial x}+\frac{\partial v}{\partial y}+\frac{\partial w}{\partial z}\right)+2\mu\frac{\partial u}{\partial x} & \mu\left(\frac{\partial u}{\partial y}+\frac{\partial v}{\partial x}\right) & \mu\left(\frac{\partial w}{\partial x}+\frac{\partial u}{\partial z}\right) \\ \mu\left(\frac{\partial u}{\partial y}+\frac{\partial v}{\partial x}\right) & \nu\left(\frac{\partial u}{\partial x}+\frac{\partial v}{\partial y}+\frac{\partial w}{\partial z}\right)+2\mu\frac{\partial v}{\partial y} & \mu\left(\frac{\partial v}{\partial z}+\frac{\partial w}{\partial y}\right) \\ \mu\left(\frac{\partial w}{\partial x}+\frac{\partial u}{\partial z}\right) & \mu\left(\frac{\partial v}{\partial z}+\frac{\partial w}{\partial y}\right) & \nu\left(\frac{\partial u}{\partial x}+\frac{\partial v}{\partial y}+\frac{\partial w}{\partial z}\right)+2\mu\frac{\partial v}{\partial z} \end{bmatrix}$$

Dynamic viscosity coefficient is determined by the following formula:

$$\frac{\mu}{\mu_0} = \left(\frac{T}{T_0}\right)^n, n = 0.76.$$

Prandtl number Pr=0.72.

Aerodynamic characteristics of the cylindrical-conical model were found [9, 10] basing on the complete unsteady Navier-Stokes equations (1) by relaxation with time. Viscous flows were calculated using the Godunov method based on Riemann problem solution. Calculation grids with number of nods higher 10^6 were generated through transfinite interpolation (2) according [9].

$$X(\xi, \eta)= \mu_1 x_{AB}(r) + \mu_2 x_{DC}(r) + \mu_3 T_1 \, dy/dr(r)_{AB} + \mu_4 T_2 \, dy/dr(r)_{DC} \quad (2)$$

$$Y(\xi, \eta)= \mu_1 y_{AB}(r) + \mu_2 y_{DC}(r) - \mu_3 T_1 \, dx/dr(r)_{AB} - \mu_4 T_2 \, dx/dr(r)_{DC}$$

Computations were conducted basing on the perfect gas model for both laminar and turbulent boundary layers in front of the separation zone. Turbulent boundary layer was modeled using the Baldwin-Lomax turbulence model and κ-ε model.

A.)

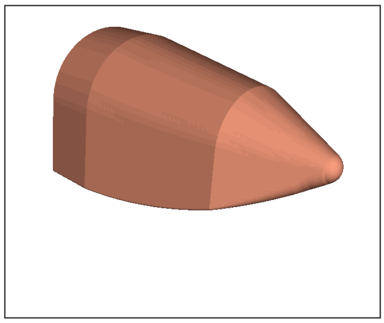

B.)

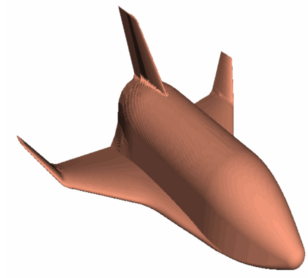

C.)

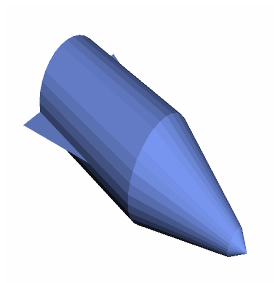

Fig.2. Three different aerodynamic schemes
A.) Lifting-body
B.) Re-entry vehicle with wing
C.) Cone-cylinder with wing

The following configurations of flight vehicle models are illustrated in Fig.2: lifting body (A), lifting body with wing (B), axisymmetric body (nose fairing) with wing (C). Estimated value of K_{max} for these configurations does not exceed K_{max}≈1,5. At the same time it is possible to obtain K_{max}≈2 if delta wing is used instead of the wing with variable sweep (configuration B) or in case of the wing with larger area for configuration C. The same value can be attained for the lifting body configuration with increased area of its lower (windward) surface. Some aerodynamic peculiarities were presented at ref. [2].

Typical flow pattern – equipressure regions – is shown in Fig. 3 for the lifting body configuration [2]. It is seen that developed high-pressure zones are realised at the windward surface of the model. Depression regions are noticed at the side surfaces and windward surface, they require mounting of additional stabilising and control surfaces (flaps, for instance) in order to provide steady flight in yaw plane.

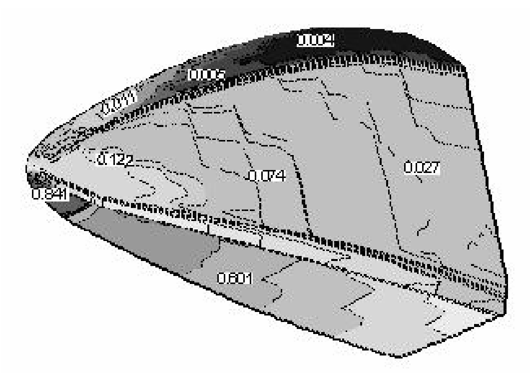

Fig.3. Typical flow pattern – equipressure regions [1].

3 Aerodynamic schemes with flight controls

Aerodynamic coefficients of the lifting body model with the flap in base region are illustrated in Fig.4 for various angles of the flap deflection. It is noted that the larger is angle of flap deflection, the less is the trimming angle of attack, and the lift-to-drag ratio dependency versus angle of attack is practically the same for examined angles of flap defection.

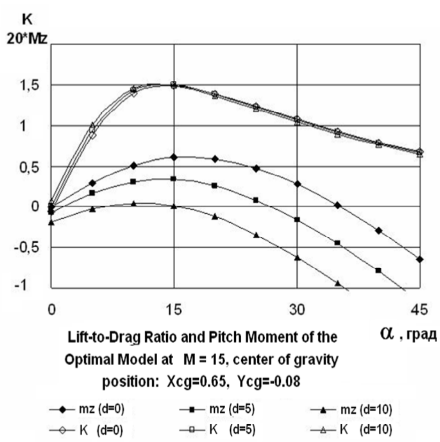

Fig.4. Lift-to-Drag ratio against angle of attack

It was found by numerical calculations on the lifting body model that several trimming angles of attack may take place with some regulations of flap [2]. For large angles of flap deflection the separation zones appeared before the control that can induce dynamic instability (Fig.5) [2]. Taking into consideration that such phenomena (several trimming angles of attack and dynamic instability) are inadmissible for manned flight, the numerical calculations were executed for the lifting body models with side jets as controls.

It was shown by the numerical computations that the side jets effect appropriately on the balancing dependencies and that lift-to-drag ratio can be increased at 20-40% if a concave configuration of the lower surface is used [2].

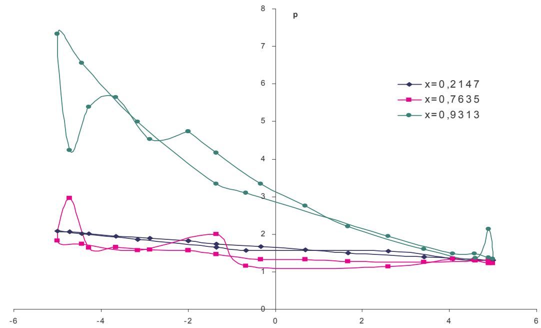

Fig.5. Pressure depending angel of attack

The article was written under support of RF President Council on Grants with research supervisor Acad. Nickolay Anfimov (НШ-2496.2008.8) and RFFI (projects ## 05-08-18034, 06-0100236).

Conclusion

The numerical simulation of hypersonic flow around vehicle models was provided for various configurations of space vehicles for manned re-entry flight. The unfavourable regimes were indicated for manned flight: two trimming angles of attack and dynamic instability of the vehicle with flaps. The side jets were suggested to provide effective and safe regimes of flight as controls with high damping capabilities.

References

[1] Ackoff R, Sasieni M. *Fundamentals of operation research*. John Wiley and sons, 1968.

[2] A. Galaktionov, V.Dineev, V.Kubyshkin, D.Fofonov *Launch vehicle last stage aerodynamics as applied to satellite injection.* The 58th IAC. 2007. India.

[3] Neyland V, Tumin A. *Aerodynamic of aero-space plane*. TSAGI, 1991.

[4] Galaktionov A.U., Lapygin V.I., Lipnitskiy U.M.. *Aerodynamic features of the hypersonic leg re-entry vehicle Kliper by type.* The 57th IAC. 2006. Spane.

[5] Galaktionov A.U., Lapygin V.I., Kazakov M.N., Mihalin V.A., Fofonov D.M. *Trade-off of aerodynamic configuration for a descent vehicle*. Brussel. 2007.

[6] Semenov Yu.P., Reshetin A.G., Dyadkin A.A., Petrov N.K., Simakova T.V., Tokarev V.A. Aerodynamic of Reentry Vehicle Clipper at Descent Phase. Proceedings of the *5th European Symposium on Aerothermodynamics for Space Vehicles*. 8-11 November 2004. SP-563. Cologne, Germany. pp.127-130

[7] Sevastiyanov N.N., Bryukhanov N.A. Clipper Reusable Transport System. *57th International Astronautical Congress*. IAC-06-D2.4.01

Copyright Statement